Modeling Chain Folding in Protein-Constrained Circular DNA

Jennifer A. Martino and Wilma K. Olson
Department of Chemistry, Rutgers, The State University of New Jersey, Wright-Rieman Laboratories, Piscataway, New Jersey 08854 USA

ABSTRACT An efficient method for sampling equilibrium configurations of DNA chains binding one or more DNA-bending proteins is presented. The technique is applied to obtain the tertiary structures of minimal bending energy for a selection of dinucleosomal minichromosomes that differ in degree of protein-DNA interaction, protein spacing along the DNA chain contour, and ring size. The protein-bound portions of the DNA chains are represented by tight, left-handed supercoils of fixed geometry. The protein-free regions are modeled individually as elastic rods. For each random spatial arrangement of the two nucleosomes assumed during a stochastic search for the global minimum, the paths of the flexible connecting DNA segments are determined through a numerical solution of the equations of equilibrium for torsionally relaxed elastic rods. The minimal energy forms reveal how protein binding and spacing and plasmid size differentially affect folding and offer new insights into experimental minichromosome systems.

INTRODUCTION

Once thought to be simply biological curiosities, minichromosomes and similar protein-wrapped DNA assemblies have become powerful tools for investigating topological change in DNA. Whether extracted from natural sources (Germond et al., 1975; Griffith, 1975) or constructed in vitro (Simpson et al., 1985; Zivanovic et al., 1988; Clark and Felsenfeld, 1992), the combination of histone protein and circular DNA provides an excellent template for investigating the tertiary structure of DNA in chromatin. Previous work has demonstrated that each nucleosome, consisting of a core of eight histone proteins bundled by ~1.75 left-handed superhelical turns of tightly associated duplex DNA, introduces significant localized elastic stress, some of which is minimized through dispersion across the entire DNA domain (Goulet et al., 1988; Yao et al., 1991; Zhang et al., 1994; Olson et al., 1996). The stress arises from the disinclination of random sequence, protein-free, double-helical DNA to bend away from an essentially linear path. Although some DNA has been shown to possess a mild, yet significant degree of intrinsic curvature (Olson and Zhurkin, 1996), at the modeling scale selected for studying global chain folding, linearity of the DNA double helix is a fair first approximation.

The consequences of extranucleosomal chain bending appear to be increasingly relevant to understanding a variety of genetic processes. For example, supercoiling has been shown to facilitate duplex strand separation for replication and transcription (Gagua et al., 1981). Chain looping can sustain local DNA architectures that bring remotely bound transcription factors into direct contact (Schild et al., 1993). Chain folding can also support interactions between regions of DNA that are remote in terms of primary structure (Paull and Johnson, 1995), potentially affording opportunities for site-specific recombination. In short, the tertiary structure of DNA may be crucial to the proper functioning of even the most elementary life forms. Minichromosomes of different chain lengths provide excellent models for the next level of DNA structural organization in eukaryotes above the (tertiary) nucleosomal wrapping of the double helix: topologically autonomous chromatin domains (Paulson and Laemmli, 1977; Marsden and Laemmli, 1979).

Recent efforts to model chain folding in minichromosomes using B-spline curves have demonstrated that the number of nucleosome complexes bound by the chain and the degree of protein-DNA interaction within each complex are important determinants of the extent of chain folding (Martino and Olson, 1997). One specific outcome is a novel resolution to the discrepancy between measured and modeled changes in linking number upon nucleosome formation. The disparity between observation and theory can arise from a variety of sources, such as the precise degree of protein-DNA interaction, the ring size, the number of bound proteins, the chain length, the protein shape, the relative protein spacing along the DNA chain, etc. Although these results point toward further investigation of the configurational impact of different minichromosome parameters, B-spline models of DNA are insufficient for such a task. These curve-fitting schemes permit small fluctuations in the total chain contour length and in the precise path and length of the model in each local, geometrically fixed portion of the chain.

To eliminate this undesirable configurational flexibility, a new approach for representing the path of the double helix through space has been implemented. The path of the DNA in each nucleosome is represented by the contour points of a left-handed superhelix of 45 Å radius and 30 Å pitch,

Received for publication 6 August 1997 and in final form 29 December 1997.

This research was presented at the DIMACS/MBBC/PMMB Workshop on DNA Topology, Rutgers University, April 1997.

Address reprint requests to Dr. Wilma K. Olson, Department of Chemistry, Rutgers University, 610 Taylor Road, Piscataway, NJ 08854-8087. Tel.: 732-445-3993; Fax: 732-445-5958; E-mail: olson@rutchem.rutgers.edu.

0006-3495/98/05/2491/10 $2.00

whereas the configurationally flexible protein-free segments of each minichromosome are modeled as elastic rods in Euler angle space. For each pair of random nucleosome locations adopted during a stochastic search, the stable configurations of the connecting sequences are determined through a numerical solution of the equations of equilibrium for elastic rods (Landau and Lifshitz, 1986). Recognizing the global minimal energy state encountered as the configuration of the complex is valid for the structures optimized, as they are essentially locked into their equilibrium states by the short, stiff, protein-free DNA linker segments they possess. Considering the wide diversity among experimentally employed minichromosome systems, the precise configurational impact of three minichromosome parameters have been explored. First, models that embody several degrees of protein-DNA interaction have been prepared to encompass the range of experimentally derived values for the nucleosome complex (Richmond et al., 1984; Furrer et al., 1995; Luger et al., 1997). Also, recent discoveries on the existence of naturally occurring nucleosome positioning sequences (Simpson and Stafford, 1983; Rhodes, 1985; Hayes et al., 1990; Thoma, 1992; Wang et al., 1994) have raised the issue of the effects of selective nucleosome deposition on the tertiary structure of DNA in closed domains. In keeping with these experimental findings, minimal energy structures of minichromosomes with a variety of core spacings have been obtained. Finally, to span a portion of the different sizes of DNA rings utilized in physical minichromosome manipulations, rings of 359 and 500 bp have been optimized. From the minimal energy structures obtained with the present algorithm, it is clear that ring size and nucleosome spacing are significant configuration-defining variables, in addition to the number of nucleosomes bound and the degree of protein-DNA interaction, previously reported (Martino and Olson, 1997). Small changes in spacing can support dramatic configurational transitions and are biologically relevant in that they determine DNA compaction and sites of inter- and intra-linker approach. In addition, the optimized configurations of the smallest rings shed light on the topological changes witnessed for comparably sized experimental systems analyzed by gel electrophoresis (Zivanovic et al., 1988). The present structures also confirm previous findings (Martino and Olson, 1997) on the nonadditivity of a popular geometric descriptor of chain folding, the writhing number.

METHODS

Minichromosome models

Identification of the minimal energy configurations of the DNA minichromosomes entails a combination of analytical and stochastic techniques. The analytical component is the solution of the equilibrium equations of the elastic protein-free DNA segments linking a given pair of nucleosomes. The stochastic element involves the search for the set of nucleosome positions in space that support the stable configuration of lowest energy. The analytical component makes use of an Euler angle representation of the tangents along the flexible DNA linker. A Cartesian coordinate representation of the complete chain is employed at the start of the search to assure the correct separations and orientations of the DNA emerging from the protein-fixed supercoils and at the finish to visualize and compute the writhing number and folding angle of the minimal energy configuration.

The Cartesian coordinates of the starting state are constructed in a piecewise manner following methodology detailed elsewhere (Martino and Olson, 1997). Briefly, pitched circular arcs and helices are generated using standard equations and spliced together using Mathematica. The smooth arcs represent the deformable protein-free DNA fragments, and the coils define the idealized superhelical paths of DNA around the nucleosome core particles (Martino, 1997). The arcs provide a useful starting point for minimization in that the protein-free DNA is fixed in an equilibrium configuration at the start. This is essential to the numerical methods employed during the random shuffling of nucleosome positions in that new equilibrium configurations are achieved by iteratively computing the corrections needed to move the current state of the system to a new spatial arrangement. This process converges only if the initial configuration is an equilibrium state not far from the new equilibrium state (Olson et al., 1996).

In contrast to our earlier B-spline optimizations, which tolerate sharp bends in the DNA as it emerges from a core particle (Martino and Olson, 1997), the present approach aligns the ends of the protein-free arcs to coincide with the DNA exiting from the flanking, fixed superhelical tracks. The equilibrium paths of the linker segments are then determined from the relative separation and orientation of the ends of the nucleosomes using the equations of equilibrium. In this way an explicit representation of the protein-bound DNA need not be maintained during the simulation. Nucleosome translations and rotations are implied throughout the stochastic search by coordinated changes in the separations and orientations of the junctions between protein-bound and free DNA segments.

The Euler angles of the tangents at the ends of the DNA linkers, $\mathbf{t}_{end} = [\sin\theta_{end}\cos\phi_{end}, \sin\theta_{end}\sin\phi_{end}, \cos\theta_{end}]$, are obtained from the Cartesian components of the abutting nucleosome tangents, $\mathbf{t}_{nucleosome} = [t_1, t_2, t_3]$: $\cos\theta_{end} = t_3$, etc. The tangents $\mathbf{t}(s)$ at other points s along the linker DNA are derived from the fundamental equation describing the equilibrium state of a thin, inextensible, twist-free, isotropic, elastic rod of circular cross section (Landau and Lifshitz, 1986):

$$EI(\mathbf{t} \times \mathbf{t}'') = \mathbf{F} \times \mathbf{t}. \tag{1a}$$

Here, E is the Young's modulus and I is the moment of a rod with tangent $\mathbf{t}$ and a constant force $\mathbf{F}$ at all points. Noting that the product EI is the coefficient of bending (A) for the rod, Eq. 1a can be expressed as

$$\mathbf{t} \times \mathbf{t}'' = \mathbf{F} \times \mathbf{t}, \tag{1b}$$

where $\mathbf{F} = [F_1, F_2, F_3]$ is the force at any point along the rod divided by EI.

Numerical solution of the equations of equilibrium

The second-order, nonlinear differential equations described by Eq. 1b are solved numerically by discretizing the rod into N subsegments of length Δs. The tangent vector along segment i is approximated by the difference in coordinates between its two ends and is expressed in the equilibrium equations in terms of Euler angles θ_i and ϕ_i:

$$\mathbf{t}_i = \begin{bmatrix} \sin\theta_i\cos\phi_i \\ \sin\theta_i\sin\phi_i \\ \cos\theta_i \end{bmatrix}. \tag{2}$$

Although the above equation is based upon the y-convention sequence of rotations (Goldstein, 1980), the results are independent of this arbitrary choice of operations provided that consistency is maintained.

The derivatives of the tangents necessary for solution of the complete set of equilibrium equations for the discretized rod,

$$\mathbf{t}_i'' = \begin{bmatrix} \theta_i''\cos\theta_i\cos\phi_i - (\theta_i')^2\sin\theta_i\cos\phi_i - 2\theta_i'\phi_i'\cos\theta_i\sin\phi_i \\ \quad - \phi_i''\sin\theta_i\sin\phi_i - (\phi_i')^2\sin\theta_i\cos\phi_i \\ \theta_i''\cos\theta_i\sin\phi_i - (\theta_i')^2\sin\theta_i\sin\phi_i + 2\theta_i'\phi_i'\cos\theta_i\cos\phi_i \\ \quad - \phi_i''\sin\theta_i\cos\phi_i - (\phi_i')^2\sin\theta_i\sin\phi_i \\ \quad - \theta_i''\sin\theta_i - (\theta_i')^2\cos\theta_i \end{bmatrix}, \tag{3}$$

are further approximated by the numerical differences:

$$\zeta_i' = \frac{\zeta_{i+1} - \zeta_{i-1}}{2\Delta s}, \tag{4a}$$

$$\zeta_i'' = \frac{\zeta_{i+1} - 2\zeta_i + \zeta_{i-1}}{\Delta s^2}, \tag{4b}$$

where $\zeta = \theta$ or ϕ.

Substitution of Eqs. 2–4 into Eq. 1b leads, after rearrangement, to $2N$ equations of the form:

$$-\frac{\theta_{i+1} - 2\theta_i + \theta_{i-1}}{\Delta s^2} + \frac{(\phi_{i+1} - \phi_{i-1})^2}{4\Delta s^2}\sin\theta_i\cos\theta_i + F_3\sin\theta_i - F_2\cos\theta_i\sin\phi_i - F_1\cos\theta_i\cos\phi_i = 0, \tag{5a}$$

$$2\left(\frac{\theta_{i+1} - \theta_{i-1}}{2\Delta s}\right)\left(\frac{\phi_{i+1} - \phi_{i-1}}{2\Delta s}\right)\sin\theta_i\cos\theta_i + \frac{\phi_{i+1} - 2\phi_i + \phi_{i-1}}{\Delta s^2}\sin^2\theta_i - F_1\sin\theta_i\sin\phi_i + F_2\sin\theta_i\cos\phi_i = 0. \tag{5b}$$

Three additional equations are invoked to maintain the spatial constraints on the ends of the DNA linkers. Both the distance between and the orientation of bound nucleosomes are assured by setting the end-to-end vector, $\mathbf{r}_N$, to the sum of displacements along the tangent vectors,

$$\sum_{i=1}^{N} \mathbf{t}_i\Delta s = \mathbf{r}_N, \tag{6}$$

and equating the end tangents, $\mathbf{t}_1$ and $\mathbf{t}_N$, to those of the flanking nucleosomes.

Newton-Raphson method

The resulting system of $2N + 3$ nonlinear equations is solved iteratively using the Newton-Raphson method. The equilibrium state of the system, $f_j(x+\Delta x)$, is expressed as a Taylor series expansion about the current state, $f_j(x)$, neglecting terms of second order or higher (Press, 1992):

$$f_j(x + \Delta x) = f_j(x) + \sum_{k=1}^{N}\left(\frac{\partial f_j}{\partial x_k}\right)\delta x_k. \tag{7}$$

Here, $f_j(x)$ is either Eq. 5a ($j = 1$) or Eq. 5b ($j = 2$), i.e., the subscript j is the equation index, whereas the x_k denote the system variables. If the partial derivatives, $\partial f_j/\partial x_k$, are equated to α_{jk} and the values of the functions describing the current state are indicated by β_j, the corrections to the variables, δx_k, which will move the function closer to zero, reduce to the unknowns in a system of linear equations,

$$\sum_{k=1}^{N} \alpha_{jk}\delta x_k = \beta_j. \tag{8}$$

In practice, $\boldsymbol{\beta}$ is a vector of order $2N + 3$ containing functional values for the two equations defining each rod subsegment (in the current state) and the three equations fixing the ends of the DNA linker. The $\boldsymbol{\alpha}$ array is constructed by substituting the current Euler variables into the derivatives of Eqs. 5 and 6 with respect to all variables (each θ_i and ϕ_i for $i = 1, N$ as well as F_1, F_2, and F_3). This matrix will be sparse owing to the dependence of each subsegment only upon its immediate neighbors (see Eqs. 3 and 4) and the independence of the end-to-end distance on components other than the θ_i and ϕ_i.

The system of linear equations is solved using Gaussian elimination in row-echelon form with back substitution (Anton, 1984) as coded by T. P. Westcott (private communication) for a condensed $\boldsymbol{\alpha}$ matrix made up of only nonzero terms. The changes in variables acquired in this manner, i.e., the set of correction values δx_k, are added to the current values stored in $\boldsymbol{\beta}$ to move the system closer to the equilibrium state (for the given set of end constraints). The elements of $\boldsymbol{\alpha}$ are retabulated based upon these revised numbers and the system of linear equations is solved again. This cycle of revising the current data and solving for the next set of corrections is repeated until the root-mean-square deviation of corrections for a given step is less than 1×10^{-6}. Beyond this point the configuration is essentially unchanged. At the end of each search, the components of the optimized loops are converted from Euler angle to Cartesian coordinate space using,

$$\mathbf{r}_{i,new} = \mathbf{r}_{i,old} + \mathbf{t}_i(s)\Delta s \tag{9}$$

where the coordinates of the curve at segment i, $\mathbf{r}_i$, are determined by analogy to the end-to-end vector (Eq. 6). Finally, the nucleosomal coils are docked onto the broken chain of linker segments.

Metropolis-Monte Carlo search of configuration space

A stochastic approach has been implemented to locate the minimal energy configurations of multiply bound DNA rings. Briefly, configuration sampling is executed via a random walk, in which a small change in nucleosome positioning is introduced, the energy of the system is calculated, and the change is either rejected or accepted according to the Metropolis criterion (Metropolis et al., 1953). The current method differs from our former explorations (Martino and Olson, 1997) in which all geometrically feasible, smoothly varying chain pathways are modeled and evaluated energetically. Here, only equilibrium (elastically stable) rod configurations are sampled and analyzed, thereby reducing the configuration search. High quality optimized structures are achieved, without the simulated annealing procedures and accelerated downhill conditioning of chain configuration demanded by explicit models of the DNA backbone (Olson and Zhang, 1991; Zhang et al., 1991).

The configurational changes consist exclusively of hypothetical nucleosome translations and rotations, as the paths of the protein-free DNA segments are completely determined by the positioning of the nucleosomes. Specifically, only the coordinates of the first and last two points of each nucleosome are maintained and moved during the simulation. (Each pair of points defines an end tangent vector of one of the connecting DNA rods.) For minichromosomes with evenly spaced proteins, translations of ±5 Å along a randomly selected global axis and rotations of ±5° about one of the same axes, are executed. Smaller increments of 2.5 Å-translations and 2.5°-rotations are used in the optimization of structures with unevenly spaced nucleosomes, as these models are configurationally constrained to a higher degree and are apt to undergo sudden elastic transitions. Because solution of the elastic equations with the Newton-Raphson technique requires the newly defined state of the system to be close to the starting

point, gradual moves are performed to dampen intrinsically sharp configurational changes.

The nucleosomes make a constant contribution to the elastic energy, but the potential of the linker DNA segments varies with nucleosome position. Their contribution to the bending energy in Euler angle space,

$$E_b = \frac{A}{2}\sum_{i=1}^{N}((\theta_i')^2 + (\phi_i')^2 \sin^2\theta_i)\Delta s, \qquad (10)$$

follows from the definition of the curvature, $\kappa = |\mathbf{t}_i'|$, with A equal to the coefficient of bending. Finally, the Boltzmann factor used by the Metropolis algorithm to determine the direction of the random walk is based on the change in total elastic energy of the constituent linkers. It is hoped that by winnowing out the higher energy structures, any solutions to the equilibrium equations that are not well stabilized will simultaneously be lost. The temperature in the Boltzmann factor is set to 120 K to generate configurational acceptance rates of 30–60%. A check is also in place to eliminate any moves that separate the nucleosomes by distances exceeding the lengths of the linker segments.

One hurdle, intrinsic to the Euler angle representation, is the indeterminate nature of some angles in selected chain orientations. Even though a configuration may be at or near its equilibrium shape, the Newton-Raphson method may register nonconvergence for a simulation move if one or more of the tangent vectors parallels the global z axis. Specifically, in defining a rotation that places the global z axis in alignment with a given tangent, ϕ can take on any value if the two axes coincide. Coding has been added to offer two possible routes out of this cul-de-sac. The first is a systematic test of the 12 possible moves for the curve (i.e., six rotations and six translations) if the initial move does not lead to solution. If none of these changes is acceptable, the entire curve is then rotated into a new spatial orientation with respect to the global frame. The former procedure skirts the problem temporarily in most cases. When neither method resolves the difficulty, the configuration is reset to the initial curve and the simulation proceeds as before. Also, if at any time the acceptance rate falls below 35% for evenly spaced nucleosomes or 15% for unevenly spaced protein constraints, the random walk is restarted. This rate is checked after every 10,000 successful moves. A simulation is also terminated if the number of unaccepted moves exceeds four times the number of successful moves for a walk.

Analysis of the global equilibrium configuration

Three quantitative descriptors of chain folding (the total bending energy, the writhing number, and a folding angle γ that describes the orientation of the bound nucleosomes in the dinucleosomal minichromosomes) are computed for each of the optimized structures. The bending energy is computed with Eq. 10 with the bending constant $A = 2.7 \times 10^{-11}$ Å-ergs, chosen to be consistent with the observed persistence length of random sequence DNA (Eisenberg, 1987; Hagerman, 1988). The writhing number is pinpointed using a new formulation developed by I. Tobias (private communication):

$$Wr = \frac{1}{2\pi}\sum_{i,j>i+1}^{N}(\Psi_{i,j} - \Psi_{i,j+1} - \Psi_{i+1,j} + \Psi_{i+1,j+1}). \qquad (11)$$

The Ψ terms in this expression correspond to the four pseudo-torsion angles defined by any pair of tangents to the curve,

$$\tan\Psi_{i,j} = \frac{(\mathbf{e}_{ij}\times\mathbf{t}_i)\cdot(\mathbf{e}_{ij}\times\mathbf{t}_j)}{\mathbf{e}_{ij}\cdot(\mathbf{t}_i\times\mathbf{t}_j)}. \qquad (12)$$

The indices of Ψ correspond to the four possible ways of joining the tangents with a straight line (i.e., head-to-head, tail-to-tail, head-to-tail, or tail-to-head), whereas $\mathbf{e}_{ij}$ is a unit vector along $\mathbf{r}_i - \mathbf{r}_j$. The folding angle is a pseudo-torsion angle set by the two positive nucleosomal axes and a virtual line connecting the centers of these phantom cores. Its computation is described in detail elsewhere (Martino and Olson, 1997).

RESULTS

Model systems

Space curves representing the central helical axis of torsionally relaxed DNA rings of different size, degree of protein-DNA interaction, and nucleosome arrangement have been simulated here. The global equilibrium structures reported in Figs. 1–4 and Table 1 reveal the extra-nucleosomal effects of the DNA-wrapping protein machine on the global tertiary structures of circular, duplex molecules.

Four series of chains have been constructed and energetically minimized. The first is a set of 500-bp dinucleosomal circular structures with evenly spaced nucleosomes binding different numbers of superhelical turns T of DNA. This and two related series of 500-bp DNAs with uneven protein spacing and variable T values provide a framework for understanding how protein binding affects global DNA configuration, whereas the final series of 359-bp dinucleosomal chains illustrates the effects of ring size on tertiary structure.

TABLE 1 Minimal energy configurations of nicked dinucleosomal DNA rings

T	Ring size	R	E_{min}	Wr	γ
1.3	500	1.00	69.3	−1.8	19
1.4	500	1.00	73.8	−1.9	30
1.5	500	1.00	78.9	−2.2	101
1.6	500	1.00	84.7	−2.9	214
1.7	500	1.00	91.2	−3.1	255
1.8	500	1.00	99.5	−3.3	318
1.9	500	1.00	110.3	−3.4	321
1.4	500	0.31	77.5	−1.9	4
1.5	500	0.31	85.4	−2.1	63
1.6	500	0.31	93.9	−2.5	81
1.7	500	0.31	99.1	−3.1	111
1.8	500	0.31	102.8	−3.3	165
1.4	500	0.15	80.1	−2.0	39
1.5	500	0.15	87.4	−1.9	117
1.6	500	0.15	92.6	−2.6	123
1.7	500	0.15	97.6	−3.0	165
1.8	500	0.15	102.3	−3.3	215
1.3	359	1.00	71.3	−1.9	30
1.4	359	1.00	74.8	−1.9	43
1.5	359	1.00	79.7	−2.1	70
1.6	359	1.00	82.7	−2.4	138
1.7	359	1.00	85.5	−2.7	195
1.8	359	1.00	93.5	−2.8	217
1.9	359	1.00	112.0	−2.8	246

T is the number of superhelical turns of DNA in the geometrically fixed coils, ring size is the DNA contour length (in bp), R is the ratio of linker lengths, E_{min} is the total bending potential (in kcal/mol), Wr is the writhing number, and γ is the folding angle (in degrees) set by the superhelical axes of the nucleosomal coils.

Minichromosomes of varied protein spacing and binding

The minimal energy configurations of 500-bp rings with two nucleosomes separated by equal linker lengths are depicted in Fig. 1, and the corresponding quantitative data are reported in Table 1. These structures offer several lines of evidence supporting their validity. For instance, the total elastic potential of these nicked minicircles increases monotonically with T (Table 1). In addition, a smooth folding progression is observed as T increases (see Fig. 1). One nucleosome flips with respect to its mate about a virtual straight line connecting their centers, giving rise to a crossover point between the linker DNA rods. This folding behavior is attested to quantitatively by concurrent decreases in the writhing numbers and increases in the folding angles (γ) of the global equilibrium curves (see Table 1). The relative rotation of the two nucleosomes can be demonstrated with a physical model of an elastic ring possessing two small, left-handed, evenly spaced coils. B-spline DNA curve representations trace similar folding pathways (Martino and Olson, 1997). Slight differences between the B-spline and elastic rod models, such as delayed or dampened folding transitions with increases in T, reflect the relaxation on the ends of the B-spline curves noted above (i.e., the ends of the protein-free chains are permitted to adopt any orientation with respect to the nucleosomal DNA). The B-spline models are also subject to uncontrolled fluctuations in chain contour length and T.

In addition to exploring how different degrees of protein-DNA interaction affect chain folding in the 500-bp ring, nucleosome spacing along the DNA chain contour has been varied. To study the configurational properties of unevenly spaced cores, which may predominate in nature, where multiple, related nucleosome positions have been identified for certain positioning sequences (Pennings et al., 1991; Meersseman et al., 1992) and weak sequence signals are easily overridden by changes in the ionic state of the environment (Blank and Becker, 1996), two families of dinucleosomal DNA rings have been optimized for two linker length ratios R. In the first case, R is set at 0.31 and T varies between 1.3 and 1.9, and in the second, $R = 0.15$ and $T =$ 1.3–1.8. The selected R values support a range of linker lengths for the shorter protein-free segment in each chain (roughly 25–65 bp) consistent with repeat lengths derived experimentally for a diverse array of organisms and cell types (van Holde, 1989), including frequently employed SV40 (~195-bp), chicken (~215-bp), and frog erythrocyte (~185-bp) DNAs. Selected minimal energy trajectories are illustrated in Figs. 2 and 3, and a quantitative analysis of all resulting configurations is presented in Table 1.

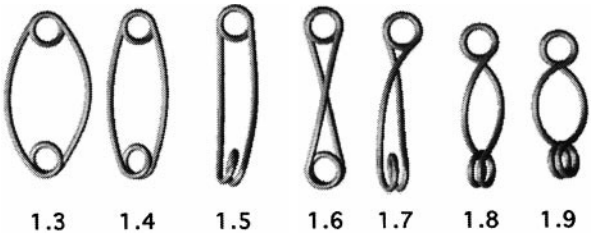

FIGURE 1 Optimized configurations of elastic rod models of 500-bp dinucleosomal DNA rings with evenly spaced bound proteins (i.e., linker length ratio $R = 1.0$). wrapping the specified number of superhelical turns of DNA around each phantom protein core. Images were created with the NDBView software package (Macskassay and Westbrook, 1997).

At first glance (see Figs. 2 and 3), the most obvious feature common to both families of unevenly spaced minichromosomes is the presence of the same chain-folding progression, observed in dinucleosomal chains of $R = 1.0$ (i.e., one nucleosome appears to flip, or rotate, with respect to the other). Although this folding event generates diverse linker segment trajectories in chains of different R, differences in the average writhe per core for a particular value of T never exceed 0.2.

Curious differences among chains of varied R but of equal T begin to emerge at $T = 1.6$. For minichromosomes with either a high or low linker length ratio (1.0 or 0.15), a linker segment crossing appears in most views of the DNA chain. However, at an intermediate value of R (0.31), there is a standoff in the elastic tug-of-war taking place between the linker segments. Neither rod can alleviate its elastic potential sufficiently to induce its partner to support a bend that yields a crossing. (When one linker segment is long, it can easily fold without introducing tremendous elastic stress, and when the two linker DNA segments are equal in length, they share whatever configurational burden is presented by the constrained DNA. However, when R is intermediate in value, neither linker DNA chain can substantially relieve the built-up elastic stress through supercoiling. Thus, chain folding appears mildly suppressed until more DNA is taken up into the core complexes.) This phenomenon is reflected in a slightly reduced writhing number (-2.5) for $R = 0.31$, at $T = 1.6$, compared with $R = 1.0$ ($Wr = -2.9$) and $R = 0.15$ ($Wr = -2.6$) (see Table 1). Once T exceeds 1.8, the formation of crossover points is independent of R, yielding an average writhe per core of -1.7.

Additional details of chain folding are revealed upon close inspection of Table 1. Clearly, although the same general chain-folding progression is observed in all 500-bp dinucleosomal rings, the evolutionary steps between $T =$ 1.4 and $T = 1.8$ are not the same. To generate twin linker segment crossings in a DNA ring of $R = 1.0$, one nucleosome must rotate ~360° relative to its sibling core on the

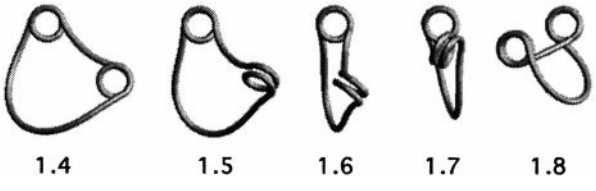

FIGURE 2 Optimized configurations of 500-bp dinucleosomal DNA rings with a linker length ratio of 0.31 for different degrees of superhelical wrapping. See legend to Fig 1.

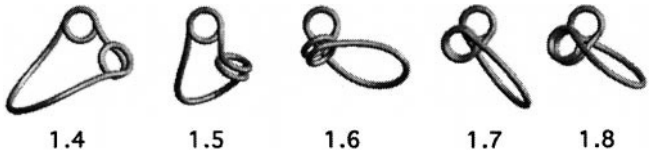

FIGURE 3 Optimized configurations of 500-bp dinucleosomal DNA rings with a linker length ratio of 0.15 for different degrees of superhelical wrapping. See legend to Fig 1.

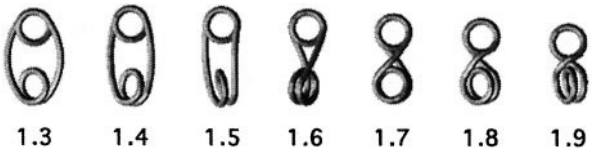

FIGURE 4 Optimized configurations of 359-bp dinucleosomal DNA rings with evenly spaced bound proteins for different degrees of superhelical wrapping. See legend to Fig 1.

same chain. For systems of $R = 0.31$ or 0.15, a single $\sim 180°$ flip of one core particle (γ) is all that is required. Also, each family of chains of distinct R value passes through an elastic transition at different values of T. For chains of $R = 1.0$ or $R = 0.15$, the largest configurational shift is manifested as T increases from 1.5 to 1.6 ($\Delta Wr = -0.7$ for both). For chains of $R = 0.31$, the main configurational transition transpires as T increases from 1.6 to 1.7 ($\Delta Wr = -0.6$).

To generalize these detailed observations into a simple idea, DNA rings with proteins separated by a very small linker on a mid-sized DNA domain (500 bp) experience dramatic configurational transitions. This may be of critical relevance to nucleosome-mediated or -activated genetic events requiring sharp configurational change (Laybourn and Kadonaga, 1992; Cullen et al., 1993; Schild et al., 1993). For example, a nucleosome positioned between the vitellogenin B1 promoter and the binding site for an estrogen receptor complex in *Xenopus* chromatin has been shown to deliver the proteins located at these two sites, (i.e., transcription factors at the B1 promoter and the estrogen receptor complex) to a common region in space for interaction that stimulates transcription of the vitellogenin gene (Schild et al., 1993). Although Schild and colleagues (1993) propose that a crossover formed by DNA emerging from the nucleosome could easily bring the transcription factors and estrogen receptor complex together in space, the presence of a second, proximally bound nucleosome, as modeled here, could provide the on-off switch for transcription. By condensing or releasing less than 10 bp of DNA from each nucleosome, the formation or dissolution of a critical linker segment crossing that draws remote proteins such as these, responsible for transcriptional activation, together in space, could be catalyzed.

Minichromosomes of miniature dimension with a range of binding

A set of 359-bp dinucleosomal minichromosomes of $R = 1.0$, where T is varied has also been prepared and analyzed. Optimized configurations for the rings are depicted in Fig. 4, and corresponding quantitative data are presented in Table 1. Notice that both 500- and 359-bp ring series follow the same folding progression with increases in T. In fact, the first three members of each wrapping progression are nearly identical in overall appearance. The magnitude of Wr and the nucleosome rotation angles γ also increase correspondingly in 500- and 359-bp chain sets alike (see Table 1).

Differences between the two families of DNA rings begin to emerge only when the linker arms of the 359-bp rings become too short to adopt low-energy trajectories as more and more DNA is taken up in the nucleosome (i.e., $T > 1.5$). This phenomenon dampens the flipping of the mobile nucleosome as T increases. For example, the first 359-bp DNA ring to exhibit a linker segment crossover midway between the two cores requires $T = 1.7$ turns of bound DNA, compared with $T = 1.6$ for the 500-bp chains. This mild retardation in the evolution of ring folding continues as T further increases and can be seen in the comparative writhing numbers and γ values provided in Table 1. Notice that the overall drop in Wr as T is increased from 1.3 to 1.9 is smaller for the 359-bp DNA ring (0.9) than for the 500-bp ring (1.6) by more than 40%. Likewise, the chain folding monitored via the rotation of the mobile nucleosome about the virtual bond connecting the centers of the two cores is also reduced for the smaller ring ($\gamma = 216°$) in comparison with the 500-bp chain ($\gamma = 302°$). To summarize, although 500- and 359-bp minichromosomes of equal T have similar configurations, the differences between the structures are significant and can be directly attributed to a change in ring size.

The choice of modeling a 359-bp chain that binds two evenly spaced phantom histone octamers was prompted by curious results obtained by Zivanovic et al. (1988) in a reconstitution experiment involving this same system. Gel electrophoresis of closed circular supercoiled chains that had been relaxed, re-ligated, and deproteinized before gel analysis supported $\Delta Lk = -1.0$ per protein. However, the geometric constraints of this system suggest that it is sterically inhibited. (The linker lengths are approximately 33 bp each, whereas the minimal through-space length of DNA required to connect the two ends of a nucleosomal supercoil along the protein surface is approximately 26 bp). This configurational inhibition supports the concept that supercoiling in such a chain should be severely hindered, thus reducing ΔLk per core. The present modeling supports this notion as the ΔWr per core in the present nicked chain models is lower in the 359-bp chain of $T = 1.7$ (-1.3) than in the 500-bp chain (-1.5). This result also reduces the former discrepancy in the values reported for ΔLk per core in reconstitution experiments (-1.0 ± 0.1) (Germond et al., 1975; Simpson et al., 1985; Zivanovic et al., 1988) versus modeling exercises (~ -1.7) (Le Bret, 1988; Zhang et al.,

1994). However, reduced linking number differences determined in reconstitution experiments (Germond et al., 1975; Simpson et al., 1985) employing DNA rings, kilobase pairs in length, remain.

DISCUSSION

Overview

The primary goals of the present investigation have been to identify configuration-determining parameters for minichromosomes and to consider how changes in these parameters may be related to biological function. In the one set of computations, minichromosomes have been optimized to investigate the structural changes introduced by salt-induced (Blank and Becker, 1996) or polymerase-directed nucleosome relocation (Studitsky et al., 1995). The second set involving 359-bp minichromosomes has aimed at exploring the properties of the small, potentially configurationally restricted minicircles, which have been used by several researchers to study specific protein-DNA interactions (Simpson et al., 1985; Goulet et al., 1988; Zivanovic et al., 1990; Kahn and Crothers, 1993; Toulm et al., 1995; Larquet et al., 1996). The understandings reaped and the questions raised in these areas are described in detail below.

RNA polymerase-directed nucleosome relocation in DNA rings

The initial intent of modeling unevenly spaced nucleosomes on a DNA template has been to examine minichromosome configurations adopted when the nucleosomes occupy more random positions along the DNA chain. Although the majority of reconstitution studies involves incorporating histone octamers into DNA rings composed of tandem repeats of DNA positioning sequences (Simpson et al., 1985; Allen et al., 1993; O'Neill et al., 1993), this method may or may not be utilized for generating arrays of nucleosomes throughout the chromatin fiber. In fact, recent investigations suggest that nucleosomes are mobile along the primary structure of DNA, thus reducing the significance of evenly spaced cores. Alterations in the temperature or ionic conditions of the immediate environment to the chromatin strand have been shown to translate cores along DNA (Pennings et al., 1991; Meersseman et al., 1992; Blank and Becker, 1996). The recent proposal made by Studitsky et al. (1995), in which a mechanism for the direct transfer of a nucleosome to locations upstream of the promoter of an active RNA polymerase is put forth, provides further fuel for the present modeling endeavors, as transcription is an ongoing necessity in the life of a cell. With the relevance of the present optimizations in sight, the biological context of the structures of Figs. 1–3 will be addressed.

As a starting point, the chains of Fig. 1 can be thought to represent small, highly simplified chromatin domains in some initial configurational state, such as that following DNA replication in which the protein constraints may be evenly spaced. Corresponding structures of equal T in Figs. 2 and 3, in which $R < 1.0$, can then provide examples of the kinds of chain deformities that would result from a polymerase transferring one of the bound core particles to a new address along the DNA chain as a direct result of transcription. For example, for a small DNA loop binding cores with $T = 1.6$, after a phantom polymerase (not shown in the figures) tracks along the DNA through the first nucleosome, the transferred histone octamer completely changes its spatial position with respect to its neighboring core, not just its location along the DNA sequence. Here the nucleosomes shift from an arrangement in which the opposite faces of the two protein cylinders share a common plane in space and are distant from each other (see Fig. 1) to a tightly packed, perpendicular arrangement of bound supercoils of DNA (see Fig. 2 or 3). The transcribing polymerase clearly wrenches the DNA minicircle into a dramatically different shape each time it delivers the core that it is transcribing through to a new upstream location. Generally, the net configurational effect of a polymerase transcribing through a nucleosome array is expected to be negligible, if all of the cores transcribed through are transferred equivalently. However, if the start and stop signals for a polymerase interrupt an array of nucleosome complexes, the configuration of the chromatin domain may be altered substantially. Such a posited structural change may even be responsible for signaling the assemblage or disassemblage of higher-order chromatin structures (e.g., the 30-nm fiber), following the genetic event.

The structures in Figs. 2 and 3 differ in the DNA chain lengths separating the nucleosomes as a result of the transcription-directed relocation of one histone octamer on a template with evenly spaced constraints. The different ratios of linker lengths, $R = 0.31$ and $R = 0.15$, offer a variety of possible minichromosome configurations potentially representative of the sampling of core relocation sites generated during transcription-catalyzed nucleosome transfer (Clark and Felsenfeld, 1992). The different degree of protein wrapping (T) introduced in the models help to visualize the likely steps involved in the spooling mechanism proposed for direct transfer of the nucleosome (Studitsky et al., 1995). During the hypothesized spooling process, some DNA unwraps from the nucleosome immediately ahead of the polymerase. In this case, the small, circular DNA chains no longer model an entire chromatin domain but represent a small portion of that domain coiled into a spooling loop that includes a single nucleosome and a DNA wrapping polymerase. Although few conclusive assertions can be made at this point regarding the precise configurations of DNA spooling loops during polymerase activity, the evidence for significant configurational distortion is apparent, even in this simplified model. Also, if more quantitative data on the transcription spooling loop or core relocation are gleaned in future experiments, three-dimensional models are already in place for detailed interpretation of such results.

Protein binding in DNA minicircles

Minicircles of a few hundred base pairs are popular tools for exploring configurational changes introduced by proteins into DNA upon complexation, as the systems are small enough to view directly using electron microscopy (EM). Recently, DNA minicircles have been bound to a variety of different proteins that bend DNA, including the histone octamer with and without the linker histone H5 (Zivanovic et al., 1988, 1990), *Escherichia coli* RNA polymerase (Kahn and Crothers, 1993), and the archaebacteria MC1 protein (Toulm et al., 1995; Larquet et al., 1996). With the association between configurational distortion and transcriptional activation growing, these studies are of great import. Thus, any additional insights provided by the present minicircle simulation studies warrant attention.

Of the complexes noted above, the reconstitution studies involving histone proteins share many of the same system parameters as those selected for the relaxed 359 bp dinucleosomal models optimized here. In fact, the system was designed with the purpose of a comparison in mind, and several revelations concerning the system have emerged. First, it is easy to account for the uncrossed configurations of the linker segments frequently observed in EM images. Previously, Zivanovic et al. (1988) argued in favor of a superhelical wrapping of under 1.5 turns of DNA per complex to account for the open configuration. They based their hypothesis on a theoretical study of a 359 bp mononucleosome which sought minimum energy, protein-free DNA loop configurations from a population of configurations generated to bind nucleosomal DNA of 43 Å radius and 27 Å pitch, with varied twists (Le Bret, 1988). The present analysis demonstrates that in a dinucleosomal system, up to 1.6 superhelical turns of DNA can be adsorbed onto the surface of each histone complex without major refolding of the minichromosome. The $T = 1.6$ value is also closer to the wrapping observed in the crystal structure of the core particle (Richmond et al., 1984; Luger et al., 1997), and nearly matches the value predicted by cryo electron microscopy analyses of core particles (Furrer et al., 1995). Although previous theoretical work on singly bound systems suggests that an elastic collapse should occur beyond $T = 1.5$ (Le Bret, 1988; Olson and Zhang, 1991), it is clear from the current simulation of dinucleosomal minichromosomes that the presence of a second protein inhibits minichromosome folding in a system so small; the result is an open chain. (The linker segments are under 50 bp each.) This may be a more accurate explanation for the unfolded chain configurations observed in electron micrographs.

Second, the present study suggests that, even if nucleosomes in natural chromatin bind in excess of 1.75 superhelical turns of DNA, this most likely would not be seen in electron micrographs of the 359-bp dinucleosomal system as the linker segments are so abbreviated that they would be in direct contact with each other and the protein-bound DNA supercoils, as demonstrated by the optimized structures presented here. As the present simulation neglects electrostatic effects, this sterically cramped configuration is allowed. However, in a charged model, fraying of DNA off of the core most likely would occur, and may have occurred in the experimental study. This possibility was not considered before. To continue this line of reasoning, if overcrowding precipitated the loss of critical histone-DNA contact sites, the reduced change in ΔLk observed in gel analyses would be consistent with this event. The overcrowding theory also provides a rationale as to why few dinucleosomal complexes form on the 359-bp ring when the linker histone H5 is present (Zivanovic et al., 1990). As H5 has been shown to extend the protein-DNA contact zone in digestion studies with micrococcal nuclease, the linker length connecting the two protein complexes would be even smaller, imposing more severe (potentially impossible) steric constraints on the system; thus, the second protein would not readily bind. In short, although minicircles provide a wealth of structural information on protein-DNA systems, they may carry configurational artifacts associated with unnaturally tight core packing.

CONCLUSIONS

Presently, two major improvements in the simulation of minichromosomes have been achieved. Although the findings of previous work employing B-spline representations of mono- and di-nucleosomal minichromosome structures are thoroughly enlightening in terms of their implications for current chromatin issues, such models tolerate a level of flexibility in fundamental system parameters that limit the identification of true global equilibrium configurations. They are also computationally expensive. Significant advances in both of these areas are reflected in the present modeling study.

First, the chain modeling technique implemented in the current study describes the trajectories of the protein-free DNA segments in terms of tangents to the central axis curve in Euler angle space. This is advantageous in that critical shape-determining parameters, such as the exact amount of DNA contacting the underlying phantom octamer and the direction of DNA emerging from the protein surface, are precisely fixed. In addition, an Euler angle description can be used to describe a wide selection of phantom protein shapes, degrees of protein-DNA interaction, and relative protein arrangement on a DNA chain. Also, the Cartesian coordinates for an optimized chain can be generated with ease and all critical topological and geometric descriptors of the complete space curve can be precisely calculated with felicity.

Second, and perhaps more significant is the present optimization algorithm itself, which solves for and examines only elastically stable configurations. With this methodology in place, configurational optimizations currently require less than 10% of the random moves necessitated by less efficient procedures to produce high quality minimal energy structures. For example, Monte Carlo protocols of B-spline

representations of chains mandated 3×10^6 to 6×10^6 moves (Martino and Olson, 1997).

Third, although applied here to the study of short, stiff, protein-free DNA linker segments that are essentially locked in their global equilibrium configurations, the elastic rod model is routinely applied to a great variety of dynamical problems in engineering mechanics. The current description of DNA in terms of the tangents of the elastic rod, however, does not consider the fluctuations of twist known to be important for nonequilibrium states (Antman, 1995). Future extensions of this work, which keep track of both the smooth bending and local helical twist of the rod, will allow us to investigate the barriers impeding transitions between competing three-dimensional minima, such as the open and closed states of symmetrically positioned nucleosome cores found by varying the degree of wrapping of DNA around protein.

Finally, although the small set of structures optimized here are rich in insights into the tertiary structures of minichromosomes, with several implications for genetic control, many chromatin-related issues remain unresolved. On-going research in the area focuses on investigating folding motifs for packaging arrays of nucleosomes into higher-order structures, identifying potential mechanisms for activation of genetic domains, as well as exploring the effects of linker length variability on higher-level chromatin organization. The ensemble of modeling and optimization techniques currently presented, however, provide a venue for successfully optimizing other structures that address these issues. Additionally, these same methods possess sufficient flexibility to enable the representation of the minimal energy configurations of a wide range of circular DNA chains bound to a diverse spectrum of trajectory-altering, DNA-binding proteins, especially those associated with transcription activities.

We are very grateful to Dr. Irwin Tobias for suggesting the current approach to modeling DNA and for providing important insights into the equations of equilibrium for elastic rods. We also thank Dr. Timothy P. Westcott for generously supplying essential FORTRAN subroutines that enable the solution of large systems of linear equations through efficient data storage. Finally, we acknowledge Dr. A.R. Srinivasan, Dr. John D. Westbrook, and Mr. Andrew J. Olson for their kind assistance in the preparation of minichromosome figures.

This research was generously supported by the U.S. Public Health Service under research grant GM34809. J.A. Martino was a Howard Hughes Medical Institute predoctoral fellow in the biological sciences at the time this work was conducted. Calculations were performed at the Rutgers University Center for Computational Chemistry.

REFERENCES

Allen, M. J., X. F. Dong, T. E. O'Neill, P. Yau, S. C. Kowalczykowski, J. Gatewood, R. Balhorn, and E. M. Bradbury. 1993. Atomic force microscope measurements of nucleosome cores assembled along defined DNA sequences. *Biochemistry*. 32: 8390–8396.

Antman, S. S. 1995. Nonlinear Problems of Elasticity. Springer-Verlag, New York.

Anton, H. 1984. Elementary Linear Algebra. John Wiley & Sons, New York. 1–56.

Blank, T. A., and P. B. Becker. 1996. The effect of nucleosome phasing sequences and DNA topology on nucleosome spacing. *J. Mol. Biol.* 260:1–8.

Clark, D. J., and G. Felsenfeld. 1992. A nucleosome core is transferred out of the path of a transcribing polymerase. *Cell*. 71:11–22.

Cullen, K. E., M. P. Kladde, and M. A. Seyfred. 1993. Interaction between transcription regulatory regions of prolactin chromatin. *Science*. 261: 203–206.

Eisenberg, H. 1987. DNA flexing, folding, and function. *Acc. Chem. Res.* 20:276–282.

Furrer, P., J. Bednar, and J. Dubochet. 1995. DNA at the entry-exit of the nucleosome observed by cryoelectron microscopy. *J. Struct. Biol.* 114: 177–183.

Gagua, A. V., B. N. Belintsev, and Y. L. Lyubchenko. 1981. Effect of base pair stability on the melting of superhelical DNA. *Nature*. 297:662–663.

Germond, J. E., B. Hirt, P. Oudet, M. Gross-Bellard, and P. Chambon. 1975. Folding of the DNA double helix in chromatin-like structures from simian virus 40. *Proc. Natl. Acad. Sci. U.S.A.* 72:1843–1847.

Goldstein, H. 1980. Classical Mechanics. Addison Wesley, Reading, MA. 128–187.

Goulet, I., Y. Zivanovic, A. Prunell, and B. Rvet. 1988. Chromatin reconstitution on small DNA rings. *J. Mol. Biol.* 200:253–266.

Griffith, J. D. 1975. Chromatin structure: deduced from a minichromosome. *Science*. 187:1202–1203.

Hagerman, P. J. 1988. Flexibility of DNA. *Annu. Rev. Biophys. Biophys. Chem.* 17:265–286.

Hayes, J. J., T. D. Tullius, and A. P. Wolffe. 1990. The structure of DNA in a nucleosome. *Proc. Natl. Acad. Sci. U.S.A.* 87:7405–7409.

Kahn, J. D., and D. M. Crothers. 1993. DNA bending in transcription initiation. *Cold Spring Harbor Symp. Quant. Biol.* 57:115–122.

Landau, L. D., and E. M. Lifshitz. 1986. Theory of Elasticity. Pergamon, Oxford. 38–86.

Larquet, É., É. Le Cam, A. Fourcade, F. Culard, P. Furrer, and É. Delain. 1996. Complméntarité des microscopies dans l'analyse structurale de minicercles d'ADN associés a la protéine MC1. *C.R. Acad. Sci. Paris*. 319:461–471.

Laybourn, P. J., and J. T. Kadonaga. 1992. Threshold phenomena and long-distance activation of transcription by RNA polymerase. *Science*. 257:1682–1684.

Le Bret, M. 1988. Computation of the helical twist of nucleosomal DNA. *J. Mol. Biol.* 200:285–290.

Luger, K., A. W. Mäder, R. K. Richmond, D. F. Sargent, and T. J. Richmond. 1997. Crystal structure of the nucleosome core particle at 2.8 Å resolution. *Nature.* 389:251–260.

Macskassay, S., and J. D. Westbrook. 1997. NDBView: a specialized 3-dimensional display program for crystallographic structures of nucleic acids, version 4.2. Rutgers University, New Brunswick, NJ. Program No. NDB-305.

Marsden, M. P. F., and U. K. Laemmli. 1979. Metaphase chromosome structure: evidence for a radial loop model. *Cell*. 17:849–858.

Martino, J. A. 1997. Modeling global equilibrium configurations of protein-constrained circular DNA. Ph.D. thesis. Rutgers, The State University of New Jersey, New Brunswick, NJ.

Martino, J. A., and W. K. Olson. 1997. Modeling protein-induced configurational changes in DNA minicircles. *Biopolymers*. 41:419–430.

Meersseman, G., S. Pennings, and E. M. Bradbury. 1992. Mobile nucleosomes: a general behavior. *EMBO J.* 11:2951–2959.

Metropolis, N., A. W. Rosenbluth, M. N. Rosenbluth, A. Teller, and E. Teller. 1953. Equation of state calculations by fast computing machines. *J. Chem. Phys.* 21:1087–1092.

Olson, W. K., T. Westcott P., J. Martino A., and G.-H. Liu. 1996. Computational studies of spatially constrained DNA. *In* Mathematical Approaches to Biomolecular Structure and Dynamics. J. P. Mesirov, K. Schulten, and D. W. Sumners, editors. Springer-Verlag, New York. 195–218.

Olson, W. K., and P. Zhang. 1991. Computer simulation of DNA supercoiling. *Methods Enzymol.* 203:403–432.

Olson, W. K., and V. B. Zhurkin. 1996. Twenty years of DNA bending. *In* Biological Structure and Dynamics, Vol. 2. R. H. Sarma and M. H. Sarma, editors. Adenine Press, Schenectady, NY. 341–370.

O'Neill, T. E., J. G. Smith, and E. M. Bradbury. 1993. Dissociation is not required for transcript elongation through arrays of nucleosome cores by phage T7 RNA polymerase in vitro. *Proc. Natl. Acad. Sci. U.S.A.* 90:6203–6207.

Paull, T. T., and R. C. Johnson. 1995. DNA looping by *Saccharomyces cerevisiae* high mobility group proteins NHP6A/B. *J. Biol. Chem.* 270: 8744–8754.

Paulson, J. R., and U. K. Laemmli. 1977. The structure of histone-depleted metaphase chromosomes. *Cell*. 12:817–828.

Pennings, S., G. Meersseman, and E. M. Bradbury. 1991. Mobility of positioned nucleosomes on 5S rDNA. *J. Mol. Biol.* 220:101–110.

Press, W. H. 1992. Numerical Recipes in Fortran: The Art of Scientific Computing. Cambridge University Press, New York,

Rhodes, D. 1985. Structural analysis of a triple complex between the histone octamer, a *Xenopus* gene for 5S RNA and transcription factor IIIA. *EMBO J.* 4:3473–3482.

Richmond, T. J., J. T. Finch, B. Rushton, D. Rhodes, and A. Klug. 1984. Structure of the nucleosome core particle at 7 Å resolution. *Nature*. 311:532–537.

Schild, C., F.-X. Claret, W. Wahli, and A. P. Wolffe. 1993. A nucleosome-dependent static loop potentiates estrogen-regulated transcription from the *Xenopus* vitellogenin B1 promoter in vitro. *EMBO J.* 12:423–433.

Simpson, R. T., and D. W. Stafford. 1983. Structural features of a phased nucleosome core particle. *Proc. Natl. Acad. Sci. U.S.A.* 80:51–55.

Simpson, R. T., F. Thoma, and J. M. Brubaker. 1985. Chromatin reconstituted from tandemly repeated cloned DNA fragments and core histones: a model system for study of higher order structure. *Cell*. 42:799–808.

Studitsky, V. M., D. J. Clark, and G. Felsenfeld. 1995. Overcoming a nucleosomal barrier to transcription. *Cell*. 83:19–27.

Thoma, F. 1992. Nucleosome positioning. *Biochem. Biophys. Acta.* 1130: 1–19.

Toulm, F., É. Le Cam, C. Teyssier, É. Delain, P. Sautiere, J.-C. Maurizot, and F. Culard. 1995. Conformational changes of DNA minicircles upon the binding of the archaebacterial histone-like protein MC1. *J. Biol. Chem.* 270:6286–6291.

van Holde, K. E. 1989. Chromatin. Springer-Verlag, New York.

Wang, Y.-H., S. Amirhaeri, S. Kang, R. D. Wells, and J. D. Griffith. 1994. Preferential nucleosome assembly at DNA triplet repeats from the myotonic dystrophy gene. *Science*. 265:669–671.

Yao, J., P. T. Lowary, and J. Widom. 1991. Linker DNA bending induced by the core histones of chromatin. *Biochemistry*. 30:8408–8414.

Zhang, P., W. K. Olson, and I. Tobias. 1991. Accelerated record keeping Fourier series Monte Carlo simulations of an isotropic elastic rod model of DNA. *Comput. Polymer Sci.* 1:3–17.

Zhang, P., I. Tobias, and W. K. Olson. 1994. Computer simulation of protein-induced structural changes in closed circular DNA. *J. Mol. Biol.* 242:271–290.

Zivanovic, Y., I. Douband-Goulet, P. Schultz, E. Stofer, P. Oudet, and A. Prunell. 1990. Chromatin reconstitution on small DNA rings: histone H5 dependence of DNA supercoiling in the nucleosome. *J. Mol. Biol.* 214:479–495.

Zivanovic, Y., I. Goulet, B. Rvet, M. Le Bret, and A. Prunell. 1988. Chromatin reconstitution on small DNA rings. II. DNA supercoiling on the nucleosome. *J. Mol. Biol.* 200:267–290.